



Spatial patterns and controls of soil chemical weathering rates along a transient hillslope

Kyungsoo Yoo^{a,b,*}, Simon Marius Mudd^c, Jonathan Sanderman^d, Ronald Amundson^e, Alex Blum^f

^a Dept. of Plant and Soil Sciences, University of Delaware, United States

^b Dept. of Geological Sciences, University of Delaware, United States

^c School of GeoSciences, University of Edinburgh, UK

^d CSIRO Land and Water, Australia

^e Division of Ecosystem Sciences, University of California at Berkeley, United States

^f United States Geological Survey, United States

ARTICLE INFO

Article history:

Received 2 June 2009

Received in revised form 4 September 2009

Accepted 8 September 2009

Available online 13 October 2009

Editor: R.W. Carlson

Keywords:

weathering

erosion

soil geochemistry

hillslope processes

sediment transport

channel incision

ABSTRACT

Hillslopes have been intensively studied by both geomorphologists and soil scientists. Whereas geomorphologists have focused on the physical soil production and transport on hillslopes, soil scientists have been concerned with the topographic variation of soil geochemical properties. We combined these differing approaches and quantified soil chemical weathering rates along a grass covered hillslope in Coastal California. The hillslope is comprised of both erosional and depositional sections. In the upper eroding section, soil production is balanced by physical erosion and chemical weathering. The hillslope then transitions to a depositional slope where soil accumulates due to a historical reduction of channel incision at the hillslope's base. Measurements of hillslope morphology and soil thickness were combined with the elemental composition of the soil and saprolite, and interpreted through a process-based model that accounts for both chemical weathering and sediment transport. Chemical weathering of the minerals as they moved downslope via sediment transport imparted spatial variation in the geochemical properties of the soil. Inverse modeling of the field and laboratory data revealed that the long-term soil chemical weathering rates peak at $5\text{ g m}^{-2}\text{ yr}^{-1}$ at the downslope end of the eroding section and decrease to $1.5\text{ g m}^{-2}\text{ yr}^{-1}$ within the depositional section. In the eroding section, soil chemical weathering rates appear to be primarily controlled by the rate of mineral supply via colluvial input from upslope. In the depositional slope, geochemical equilibrium between soil water and minerals appeared to limit the chemical weathering rate. Soil chemical weathering was responsible for removing 6% of the soil production in the eroding section and 5% of colluvial influx in the depositional slope. These were among the lowest weathering rates reported for actively eroding watersheds, which was attributed to the parent material with low amount of weatherable minerals and intense coating of the primary minerals by secondary clay and iron oxides. We showed that both the morphologic disequilibrium of the hillslope and the spatial heterogeneity of soil properties are due to spatial variations in the physical and chemical processes that removed mass from the soil.

© 2009 Elsevier B.V. All rights reserved.

1. Introduction

Some of the major challenges in Earth science are to understand the complex feedbacks between the tectonic and climatic forcings, geomorphic and geochemical processes, and morphological and geochemical properties of landscapes. Unraveling this complex web has far reaching implications. Tectonic uplift is considered to be intimately linked to enhanced silicate weathering, which affects the drawdown of atmospheric CO_2 (Raymo and Ruddiman, 1992; Berner,

1995). In this hypothesis, the ability of tectonic uplift to drawdown CO_2 hinges on the rates of geochemical reactions taking place within eroding landscapes. In addition, mineral exposure by uplift and erosion is required for chemical weathering to proceed which is crucial for releasing inorganic nutrients that help drive the biogeochemical cycles of the Earth (Porder et al., 2005, 2007).

Soil mantled hillslopes provide a convenient observational setting to unravel the complex mechanisms and feedbacks using a quantitative, process-based approach. Over the past century, two disciplinary groups have studied soil mantled hillslopes from significantly differing perspectives, and the resulting disciplinary gap has hindered integration of the largely complementary approaches (Anderson et al., 2007; Humphreys and Wilkinson, 2007; Yoo and Mudd, 2008a). Geomorphologists have focused largely on hillslope physical processes, revealing that the surface horizons of soils are “conveyor belts” which transport

* Corresponding author. Dept. of Plant and Soil Sciences, University of Delaware, United States.

E-mail addresses: kyoo@udel.edu (K. Yoo), simon.m.mudd@ed.ac.uk (S.M. Mudd), jonathan.sanderman@csiro.au (J. Sanderman), earthy@berkeley.edu (R. Amundson), aebalum@usgs.gov (A. Blum).

soil material downslope. Many feedbacks occur within this conveyor system. Any increase in channel incision at the base of a hillslope leads to steeper gradients, which in turn accelerates the colluvial soil transport. The increased soil transport will propagate upslope, which in turn causes soil thinning (Furbish and Fagherazzi, 2001; Mudd and Furbish, 2005). Soil thinning typically leads to increased soil production (Heimsath et al., 1997), which in turn replaces the thinning soil and thus the hillslope evolves toward a new steady state soil mantle and, over long time periods, morphology. Based on early analyses of the convexity of hillslopes (Davis, 1892; Gilbert, 1909), the morphologic evolution of hillslopes has been considered the result of physical soil production and soil transport (Fernandes and Dietrich, 1997; Roering et al., 1999; Dietrich et al., 2003). Only a few studies have recently begun to incorporate chemical weathering as a process that sculpts landscapes in non-karst terrain (eg., Anderson et al., 2002; Riebe et al., 2004; Mudd and Furbish, 2004).

In contrast, the majority of soil scientists and geochemists have focused on chemical processes in soils. To determine weathering rates, chronosequences of soils (similar climate, parent material, biota but differing ages) are studied. The mass loss via chemical weathering in each soil can be determined using geochemical comparison of the soil to its parent material (Brimhall and Dietrich, 1987). This mass loss can be converted into a chemical weathering rate by dividing it by the soil age which is defined as the time since the cessation of either erosion or deposition (Amundson, 2004; Yoo and Mudd, 2008b). On hillslopes, however, soil age cannot be defined because erosion continues to rejuvenate the soil material. This necessitates an alternative means of quantifying time within eroding soils. An additional but rarely studied complication is that a soil at a given topographic position is made not only of material from the underlying parent material, but is also comprised of material eroded from upslope. Due to these complications there has been little progress in deciphering spatially variable rates of soil chemical weathering within morphologically dynamic landscapes. Indeed, the common description of upland soils as “residual” reflects the historical neglect of physical transport by many soil scientists.

It is clear that both geochemical and geomorphic processes shape soil mantled hillslopes simultaneously. The impact of topography-dependent chemical weathering on the morphologic evolution of hillslopes has been theoretically explored (Mudd and Furbish, 2004), and studies of the topographic variation of soil geochemistry have begun to consider the geomorphic setting of the soil (Nezat, et al. 2004; Green et al., 2006; Mudd and Furbish, 2006; Yoo, et al. 2007) Two recent studies (Green, et al. 2006; Yoo, et al. 2007) combined a mass balance of hillslope sediment and soil geochemistry, and found systematic variations in chemical weathering rates along hillslope transects. Yoo et al. (2007) revealed a previously unexplored coupling between colluvial flux and chemical weathering rates, demonstrating how topographic variation of chemical weathering rates drive the chemical weathering rates at the larger scale of watersheds (Yoo, et al. 2007; Yoo and Mudd, 2008a).

This study expands on these recent studies in three ways. Previous models have been derived for steady state soil mantled slopes (Yoo et al., 2007). Here, we include a new time-dependent mass balance to examine a depositional hillslope. Second, we begin to elucidate the mechanisms that control the topography-dependent soil chemical weathering rates. Lastly, we extend previous studies' focus on granitic landscapes to hillslopes underlain by sedimentary sandstone.

2. Conceptual framework

We have derived equations of mass conservation wherein the rate of mass loss due to chemical weathering from a soil is proportional to two mineral supply rates: colluvial soil input from upslope and soil production from the underlying saprolite (Figs. 1 and 2). For a steady state soil on a hillslope, the total chemical weathering rate (all

elements) and the chemical weathering rate of an individual element, j , can be represented in the following equations. For a detailed derivation of the mass balance equations, see Yoo and Mudd (2008a) and Yoo et al. (2007).

$$W_{\text{total}} = -\frac{\nabla C_{i,s}}{C_{i,s}} \cdot (\rho_s Q_s) - \rho_{\eta} \left(1 - \frac{C_{i,\eta}}{C_{i,s}}\right) P, \quad (1a)$$

and

$$W_j = \left(1 - \frac{C_{j,\eta}}{C_{j,s}}\right) (C_{j,\eta} \rho_{\eta} P) + \left(\frac{\nabla C_{i,s}}{C_{i,s}} - \frac{\nabla C_{j,s}}{C_{j,s}}\right) \cdot (C_{j,s} \rho_s \tilde{Q}_s), \quad (1b)$$

where W is the chemical weathering loss (negative) or gain (positive) rate [$\text{kg m}^{-2} \text{yr}^{-1}$], ρ is bulk density [kg m^{-3}], P is the rate of soil production, defined as the lowering rate of the soil–saprolite interface [m yr^{-1}], \tilde{Q}_s is the volume of colluvium crossing a contour line of unit length per time [$\text{m}^2 \text{yr}^{-1}$], h is the soil thickness [m], the subscript s represents colluvial soil, the subscript η represents the values of the saprolite at its interface to the colluvial soil, and the gradients of elemental concentrations (∇C) represent the rates that the concentrations vary per unit length along the hillslope transect. The physical flux of colluvial soil can be calculated by integrating the excess of soil production rate over chemical weathering rate in the upslope area:

$$|\tilde{Q}_s|_x = (P_x - W_x) dx + \alpha_x |\tilde{Q}_s|_{x-dx}, \quad (2)$$

Where α_x is the ratio of the contour lengths ($l_{x-\Delta x}/l_x$ in Fig. 1c). The value of α_x is 1 on planar slope, <1 on horizontally divergent slope, and >1 on horizontally convergent slopes.

We calculated the soil production rate as a function of position using measurements of soil thickness and the relationship between soil thickness and soil production reported at this site by Heimsath et al. (1997). This information, as well as the elemental concentrations in the colluvial soil and saprolite, was used in Eqs. (1a), (1b) and (2) to simultaneously calculate the colluvial flux and the total weathering rate of the soil and of its individual elements (Yoo et al., 2007). The calculations require an iterative technique: the total weathering rate was first calculated using Eq. (1a) based on an arbitrary colluvial flux rate, and the resulting chemical weathering rate was inserted into Eq. (2) in order to solve for the colluvial flux rates. This process was repeated until the changes in weathering and physical flux rates between iterations became insignificant. This method does not require a specific mathematical form for the soil transport (e.g. a slope-dependent versus a soil thickness–slope product soil transport law as in Dietrich et al., 2003; Heimsath et al., 2005) because colluvial flux is, by definition, the integral of the soil produced upslope minus the mass lost chemically upslope of a given point. Though this paper focuses on chemical weathering, this iterative technique was also used to demonstrate the slope–depth dependency of colluvial flux (Yoo et al., 2007).

In some portions of the landscape, or indeed throughout entire landscapes, soil production may not be balanced by erosion and chemical weathering. This leads to transient thinning or thickening of the soil and is often caused by changes in the rate of incision or deposition in the channel at the base of the hillslope. As we will show later in this paper, the hillslope examined here is at or near steady state in its upper eroding portion, but is in a transient state in the lower depositional area. For this depositional hillslope, we developed a simplified mass balance which does not require the steady state assumption. Fig. 2 describes a depositional section of a hillslope where mass balance is largely determined by colluvial accumulation. The depositional section begins where the slope curvature shifts from convexity to concavity and extends to the hillslope–channel (or hollow axis) boundary. It is assumed that the colluvial loss from this

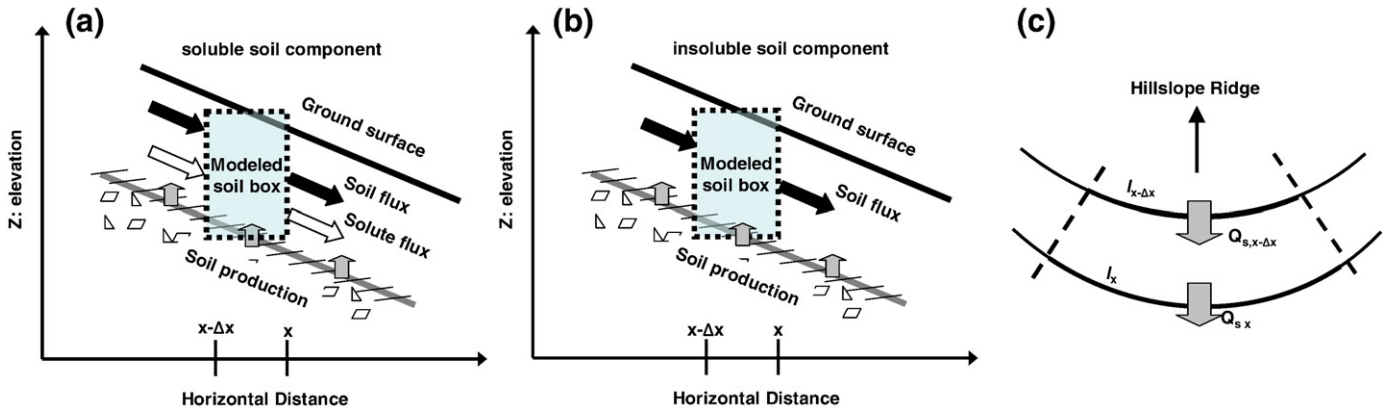


Fig. 1. Solid and solute mass fluxes on hillslope soils: (a) mass fluxes of dissolvable soil materials in and out of a modeled soil system, (b) mass fluxes of an insoluble soil component, and (c) plan view of colluvial soil flux (from Yoo et al., 2007).

area is negligible relative to the colluvial input. The mass balance of depositional soil (Eq. (3a)), immobile elements (Eq. (3b)), and an element j (Eq. (3c)) can be constructed for this section of hillslope as:

$$\langle \rho_s \rangle \langle \tilde{Q}_{sl} \rangle T = \bar{\rho}_s \bar{h}_{s,dep} (L-l) + \langle W_{total,dep} \rangle (L-l) T, \quad (3a)$$

$$\langle \rho_s \rangle \langle C_{i,s,l} \rangle \langle \tilde{Q}_{sl} \rangle T = \bar{\rho}_s \bar{C}_{i,s,dep} \bar{h}_{s,dep} (L-l), \quad (3b)$$

and

$$\langle \rho_s \rangle \langle C_{j,s,l} \rangle \langle \tilde{Q}_{sl} \rangle T = \bar{\rho}_s \bar{C}_{j,s,dep} \bar{h}_{s,dep} (L-l) + \langle W_{j,dep} \rangle (L-l) T. \quad (3c)$$

The bracketed terms represent the time-averaged values during the accumulation of the depositional soil. T represents the time length of the accumulation which is obtained by dividing the mass of deposited sediment by the sediment influx from the upslope area. The time-dependent behavior of chemical weathering during the deposition is beyond the scope of this work. Unlike in the steady-state hillslope where the chemical weathering rate is calculated as a continuous function of hillslope positions, in the depositional hillslope the calculated chemical weathering rates (terms with upper bars in Eqs. (3a)–(3c)) are values averaged over the depositional area. The term l represents the distance from the hillslope ridge to the point where the transition from steady state to transient areas occurs, and L represents the distance from the ridge to the lower end of the hillslope or the channel, and subscript dep represents the depositional transient component of the hillslope. Rearranging Eqs. (3a)–(3c), we find that

the total and elemental chemical weathering rates of the transient hillslope are described as:

$$\langle W_{total,dep} \rangle = \left(1 - \frac{C_{i,s,l}}{\bar{C}_{i,s,dep}} \right) \frac{\rho_s \tilde{Q}_{s,l}}{(L-l)}, \quad (4a)$$

and

$$\langle W_{j,dep} \rangle = \left(C_{j,s,l} - \frac{\bar{C}_{j,s,dep}}{\bar{C}_{i,s,dep}} C_{i,s,l} \right) \frac{\rho_s \tilde{Q}_{s,l}}{(L-l)}. \quad (4b)$$

3. Study site and laboratory analysis

We investigated a grass covered hillslope in the Tennessee Valley located in coastal California (Fig. 3). Mean annual rainfall is roughly 1100 mm, and the mean annual temperature is 14 °C (NCDC, 2007). At this site, the generation of mobile colluvial soil and its downslope transport are largely mediated by burrowing pocket gophers (*Thomomys bottae*) (Black and Montgomery, 1991; Heimsath et al., 1997; Yoo et al., 2005b). The rate of soil production at Tennessee Valley decreases exponentially with increasing soil thickness (Heimsath et al., 1997). Quantification of long-term fluxes indicates that colluvial soil flux is proportional to the product of slope gradient and soil thickness (Heimsath et al., 2005; Yoo et al., 2005b). The region is vegetated with annual and perennial grasses, with a discontinuous cover of coyote brush (*Baccharis pilularis*), which has been expanding across the landscape from the depositional hollows since grazing ceased in 1982 (O'Farrell et al., 2007). The Tennessee Valley is underlain by a mixture of Franciscan greywacke sand stone, serpentines, and chert (Wahrhaftig, 1984), which is to some degree visually manifested in the topography and the rockiness of the soils. The site is located near the San Andreas Fault, and the area has been exposed to a complex tectonic history associated with the lateral faults and uplift (Wakabayashi, 1999).

We selected a well defined smooth hillslope transect that stretched from a convex or eroding summit to a convergent or depositional footslope. The hillslope's lower boundary is set by an ephemeral 1st order channel; flow in the channel is generally confined to wet winter months. Our lowermost soil pit was water saturated during our sampling efforts in March 2005, which contrasts with the soils at shoulder and planar slope positions that remained well drained. This indicates dramatically different soil moisture conditions along the hillslope (Sanderman et al., 2009). Previous studies showed that the heads of the 1st order channels in this area migrate as a function of climate (Montgomery and Dietrich, 1989; Montgomery, 1999). Near the channel, saturation overland flow can

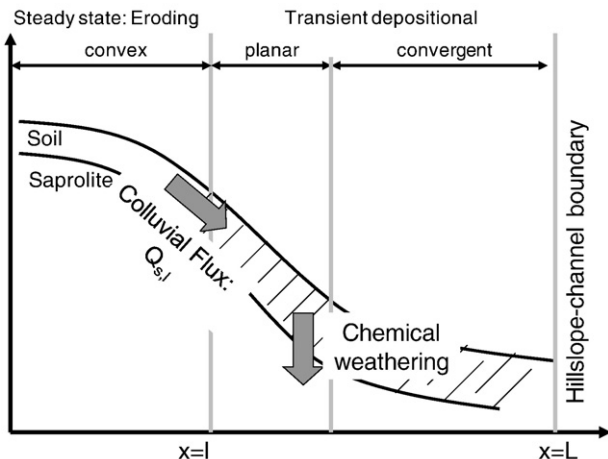


Fig. 2. Chemical and physical mass balance at the lower segments of a hillslope, which includes planar and convergent slopes.

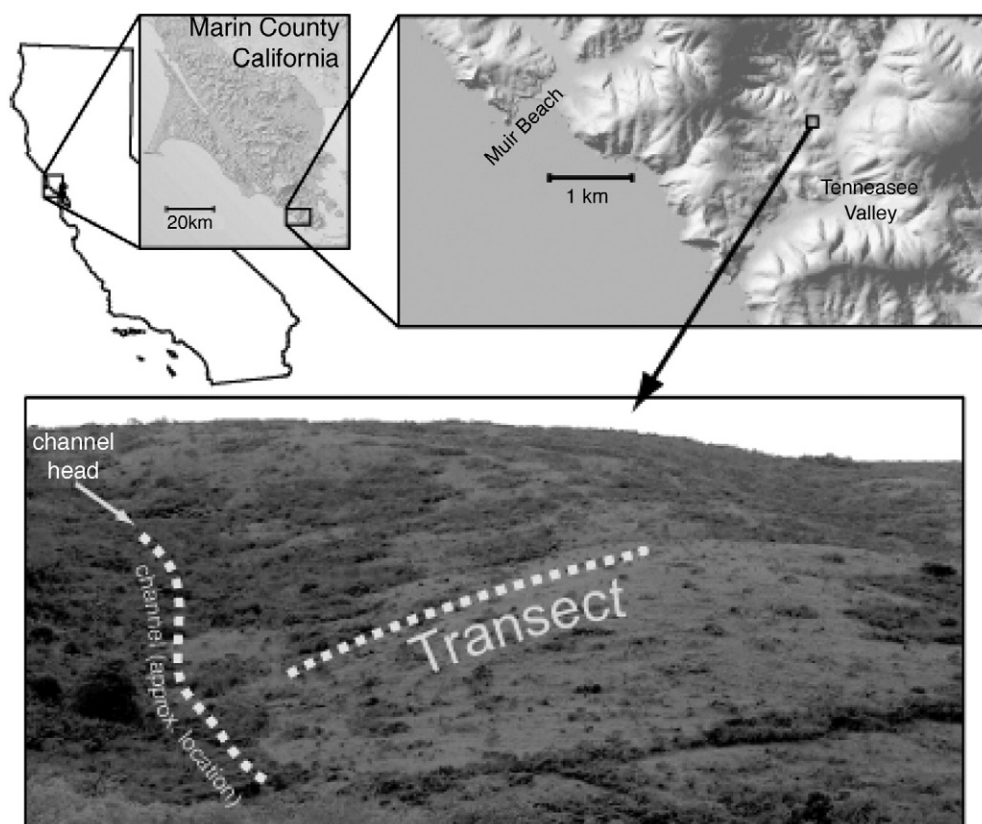


Fig. 3. Location of the study site.

develop during heavy rainfall (Montgomery and Dietrich, 1995) but overland flow results in minimal erosion due to the resistance from the grass cover (Prosser et al., 1995; Prosser and Dietrich, 1995). Reneau et al. (1990) demonstrated that the episodic landslide events occurring in unchanneled hollows were more common during the wet-to-dry climate transition in the early Holocene.

We defined soil as a physically mixed colluvial layer which is composed of A horizons at the site. Lack of physical disturbance and visual signs of rock texture in the saprolite suggests that the saprolite has been iso-volumetrically weathered. No data is available regarding the depth to fresh bedrock and its geochemistry at the site. It is unlikely that bedrock outcrops in the adjacent hillslopes, which probably survived weathering due to their distinct weathering properties, represent the fresh bedrock of the studied hillslope. Fifteen locations were chosen along a water flow line on the hillslope (Fig. 3). One location at the lowest end of the hillslope was argued due to the saturated conditions mentioned earlier. At the remaining locations, soils were excavated to a depth that extended ~30 cm beyond the boundary between soil and saprolite. At nine of the fifteen locations soils were sampled for geochemical analyses. Soil samples were collected in 5 to 15 cm depth intervals, with the highest density of samples taken near the surface. Because the physical breakdown of the saprolite is responsible for soil production, the saprolite samples used as parent material were taken near the soil-saprolite boundary. We sampled the four corners of saprolite exposed in soil pits that had basal areas of roughly ~1 m² and used their averaged elemental compositions to ascertain the local heterogeneity of the soil's parent material. Our field observation suggests that the saprolite is derived from clay-rich sandstone and is at least visually homogenous within the studied transect. Furthermore, the absence of weathering resistant rock outcrops supports the bedrock homogeneity of the studied transect. Differential GPS was used to create a topographic map of the site, and the locations of the sampling sites were mapped with sub-meter accuracy.

The soil samples were oven dried and divided into fine (<2 mm) and coarse (>2 mm) fractions using a sieve. Approximately 10 gram sub samples were taken from both size fractions of the soil samples using a splitter. Each sub-sample was then pulverized in a tungsten carbide ring using the SPEX Shatter Box for five minutes. Saprolite samples were not divided into different size fractions but were otherwise treated identically to soil samples. Pulverized samples were submitted to ALS Chemex for chemical analyses, where samples were first fused with lithium meta-borate prior to ICP-MS determination of elemental chemistry. Elemental compositions of the two soil particle size groups were combined with measured mass ratios of the fine and coarse fractions to calculate the total soil concentrations.

To investigate the mineralogical composition of the soil and saprolite, quantitative X-ray diffraction (XRD) analyses were conducted for fine and coarse fractions of soil and saprolite samples at an eroding and a depositional location within the studied hillslope. One gram of sample was ground for 5 minutes in a McCrone mill with a ZnO internal standard, then sieved and side packed in a random mount. XRD spectra were collected on a Siemens D500 instrument from 5 to 65 degrees 2 θ , with Cu K α radiation, at 0.02° step, and a two second count time. Mineral concentrations were determined using the RockJock program (Eberl, 2003), which fits the observed sample spectra as the sum of the spectra from measured mineral standards, with the fitted scaling factors for the standards reflecting the mineral abundances in the sample. The details of sample preparation and RockJock calculations are described in Eberl (2003). The accuracy and detection limits of the RockJock technique are difficult to quantify, and sample dependent. In general, the precision of an individual mineral abundance is about $\pm 5\%$ of the reported abundance. However, highly crystalline phases with little chemical variability, such as quartz, have higher precisions, while phases with highly variable chemistry and crystallinity, and minerals with diagnostic peaks in inconvenient locations, such as biotite, may have greater uncertainties.

4. Results and discussion

4.1. Geomorphic context

Three distinct zones of soil thickness and hillslope morphology can be identified at the field site (Fig. 4). The first zone, starting at the summit and extending downslope, has convex topography and little variation in soil thickness. The second zone begins ~29 m from the summit. In this zone the topography becomes planar and there is a sharp increase in soil thickness. Finally, beginning ~44 m from the summit, the topography becomes convergent with soil that is of relatively uniform thickness when compared with the planar zone but is substantially thicker than in the convex zone.

The relatively uniform soil thickness on the convex slope is indicative of steady state conditions, i.e. a condition in which soils do not thicken or thin over time. Previous investigations have suggested that convex hillslopes do not feel transient changes in the channel incision at their lower hillslope boundaries. According to Heimsath et al. (2005) and Yoo et al. (2005a,b), sediment transport at Tennessee Valley is proportional to the product of local slope and soil thickness. Based on a theoretical relationship among the timescale of eroding hillslope's morphologic adjustment to changing channel incision, the length of hillslope, and sediment flux (Mudd and Furbish, 2007), this time scale at Tennessee Valley is between ~100 ka–350 ka (the variation is due to the range in soil thickness): significantly longer than the reported time scale of ~10 ka for the cycles of hollow accumulation and evacuation which may involve channel head migration in the area (Reneau et al., 1990). Because short-term fluctuations in the rate of channel incision propagate only a short distance upslope (Furbish and Fagherazzi, 2001; Mudd and Furbish, 2005), the convex portion of the hillslope near the summit can achieve a long-term balance between soil production and both physical and chemical denudation. In contrast, the thick soils in the depositional section of the hillslope indicate that soil production is not balanced by denudation in the planar and concave zones of the hillslope, and that this transient portion of the hillslope is responding to a reduction in the rate that the channel removes colluvial soil from the base of the hillslope.

4.2. Mineralogical context

According to the quantitative XRD (electronic supplement), the abundance of minerals is similar in the soils and saprolites and between the eroding and depositional locations. This suggests that bedrock underlying the transect is relatively homogenous. Quartz was the most abundant mineral species with an average concentration of

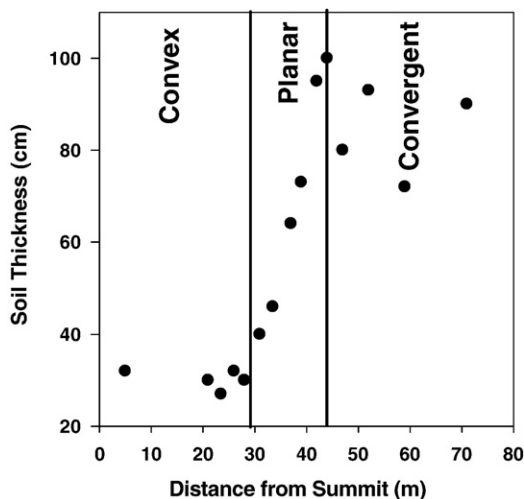


Fig. 4. Measured soil thicknesses and three morphologically distinct zones within the studied hillslope.

$40 \pm 1.0\%$ (standard error including fine and coarse soil fractions and saprolite samples $n = 24$). Another major primary mineral is plagioclase that comprises 10–20% of the samples ($14 \pm 0.5\%$). The presence of goethite is also evident ($2 \pm 0.1\%$). In total, non-clay minerals comprised 56–64% of the sample masses. The second most abundant minerals were the phyllosilicate clay minerals including mica, illite, and smectites ($24 \pm 1.0\%$). Together with kaolinite ($10 \pm 0.5\%$) and chlorite groups ($9 \pm 0.4\%$), clay minerals explain 36–45% of the total mass of soil, which agrees well with clay contents measured with hydrometer. Soil texture is clay loam to clay.

4.3. Elemental concentrations of soils and saprolites

Our mass balance calculations require the identification of a chemically immobile element to serve as an index. Zirconium was chosen as the index after comparing prospective immobile elements using the methodology of Kurtz et al. (2000). The contents of major oxides and trace elements in the soil and saprolite are presented in the electronic supplement. Continuous functional relationships were sought between the elemental concentrations and the distance from the ridge (Fig. 5). These relationships were then used in calculating chemical weathering rates using the mass balance models (Eqs. (1a)–(4b)). These empirically fitted equations can be found in the electronic supplement, and the goodness of the fits (r^2) was generally above 0.8.

In general, Zr concentrations in the soil progressively increased in the downslope direction and became spatially uniform in the convergent area of the hillslope. Saprolite Zr concentrations showed significant variations within the eroding and planar slopes but relatively uniform and higher values in the convergent area (Fig. 5a). Colluvial Zr concentrations were slightly higher or similar to the underlying saprolite values in the upper part of the hillslope. If the soil in the convergent area was formed via weathering of in-situ saprolite, the soil would have equivalent or higher Zr concentrations relative to the local saprolite. The data show, however, that Zr concentrations are greater in the saprolite compared to soil in the depositional zone of the hillslope, indicating that the soil in the depositional zone is not a weathering product of the underlying saprolite. This demonstrates that proper assessment of chemical weathering in soils on hillslopes cannot be obtained by comparing the soil and the underlying parent material: an understanding of lateral sediment transport is required to adequately interpret soil weathering history at any point on a hillslope transect.

Based on the elemental relationships between the colluvial soil and the underlying in-situ saprolite, the major oxides can be divided into three groups: (1) SiO_2 , (2) Fe_2O_3 , Al_2O_3 , K_2O , Na_2O , MgO , and (3) CaO and P_2O_5 . The concentration of SiO_2 was higher in the soil than in the underlying saprolite in the convex and planar zones of the hillslope; their values, however, converged in the depositional zone (Fig. 5b). For Fe_2O_3 , Al_2O_3 , K_2O , and Na_2O , the colluvial soils had concentrations lower than the underlying saprolites in the upper part of the hillslope (except Fe_2O_3 at the ridge) whereas the soil and saprolite show similar values in the convergent area (see electronic supplement). Calcium and P, two biologically cycled elements, were consistently enriched in the colluvial soil relative to the underlying saprolite (Fig. 5c, d). This indicates the biological uptake of Ca and P from the saprolite and subsequent retention within the soil.

4.4. Inverse modeling calculation of colluvial flux

We calculated colluvial flux along the steady state part of the hillslope (Fig. 6) using Eqs. (1a), (1b) and (2). Additionally, soil production rates were calculated from the soil thickness using the published relationship between soil thickness and soil production rate (Heimsath et al., 1997). The calculated colluvial flux across unit

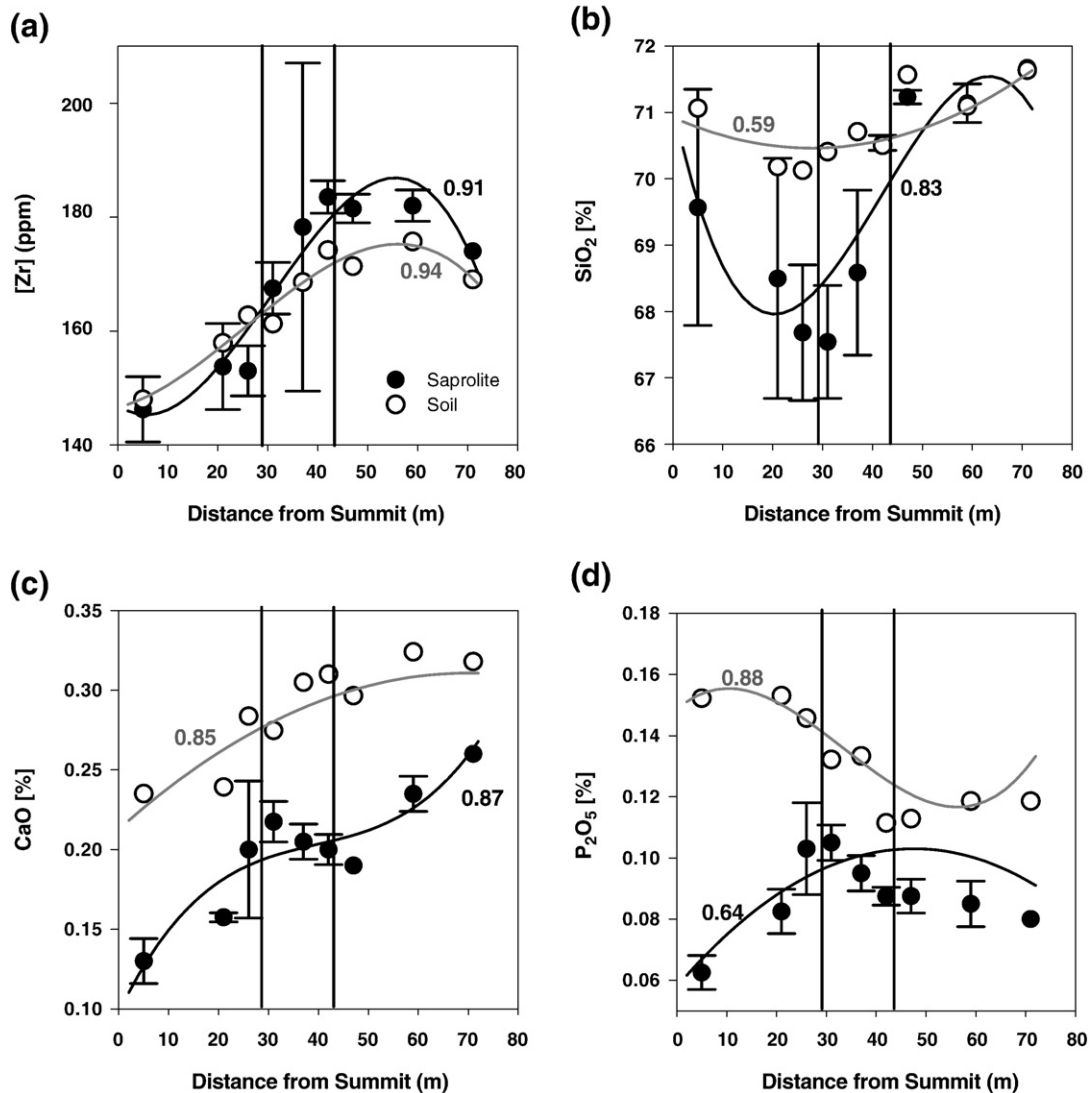


Fig. 5. Measured elemental concentrations along the hillslope transect. (a) Zr, (b) SiO_2 , (c) CaO, and (d) P_2O_5 . For the values of concentrations of all major oxides, see electronic supplement. The lines connecting the data are empirical polynomial fits that were used in calculating chemical weathering rates. The equations of polynomial fits are in the electronic supplement. The numbers represent the goodness of the fits (r^2). The vertical lines indicate the transition from convex to planar to convergent slopes.

contour length increased in the downslope direction from zero (a prescribed value) at the summit to $1.2 \text{ kg m}^{-1} \text{ yr}^{-1}$ at 30 m from the summit, where the transient slope begins. This is approximately 70% of the sediment flux estimated by the calibrated flux relationship reported by Heimsath et al. (2005). Heimsath et al. (2005) did not account for chemical weathering in their calculations, so it is not surprising that our estimate of flux is lower than the Heimsath et al. (2005) estimate. Apart from the first several meters near the summit, the colluvial flux explained more than 80% of the mass inputs to the soil columns along the eroding slope (Fig. 6b).

4.5. Inverse modeling calculation of chemical weathering rates in the colluvial soil

The mass balance calculation (Eq. (1a)) showed that within the eroding slope, the total mass loss rate via chemical weathering increased in the downslope direction reaching the maximum value of $5 \text{ g m}^{-2} \text{ yr}^{-1}$ (Fig. 7a) at the lower end of the steady state zone. The weathering rate associated with colluvial flux increased linearly in the downslope direction and increasingly dominated the total weathering loss rate (Fig. 7b). Therefore, without considering the colluvial flux and

its chemical weathering, a direct comparison of the soil to the underlying saprolite would yield spurious interpretations of weathering, which is consistent with our previous work (Mudd and Furbish, 2006; Yoo et al., 2007). In the transient slope segment (Figs. 2 and 4), the time and space averaged weathering loss rate is $1.5 \text{ g m}^{-2} \text{ yr}^{-1}$, which is less than half of the averaged rate of $3.9 \text{ g m}^{-2} \text{ yr}^{-1}$ within the eroding slope (Fig. 7a).

The trends in the weathering rates of three most abundant elements, Si, Al, and Fe (Fig. 7c) are similar to the trend in the total chemical weathering rate. Considering that the total weathering loss rate includes the loss of oxygen ions, the sum of the elemental weathering rates of Si, Al, and Fe was in a good agreement with the independently calculated total chemical weathering rates (using only Zr). One puzzling result, however, was that the summit soil showed Fe accumulation at a rate of $\sim 0.7 \text{ g m}^{-2} \text{ yr}^{-1}$. Though we do not have data to explain this result, during our sampling, we found that the summit soil was filled with water for several days after a storm, which contrasted with rapid drainage of other soils in the convex and planar slope. Such temporary saturation may have resulted in the reduction of Fe+3 to +2 and the introduction of the reduced Fe from the saprolite to the overlying soil.

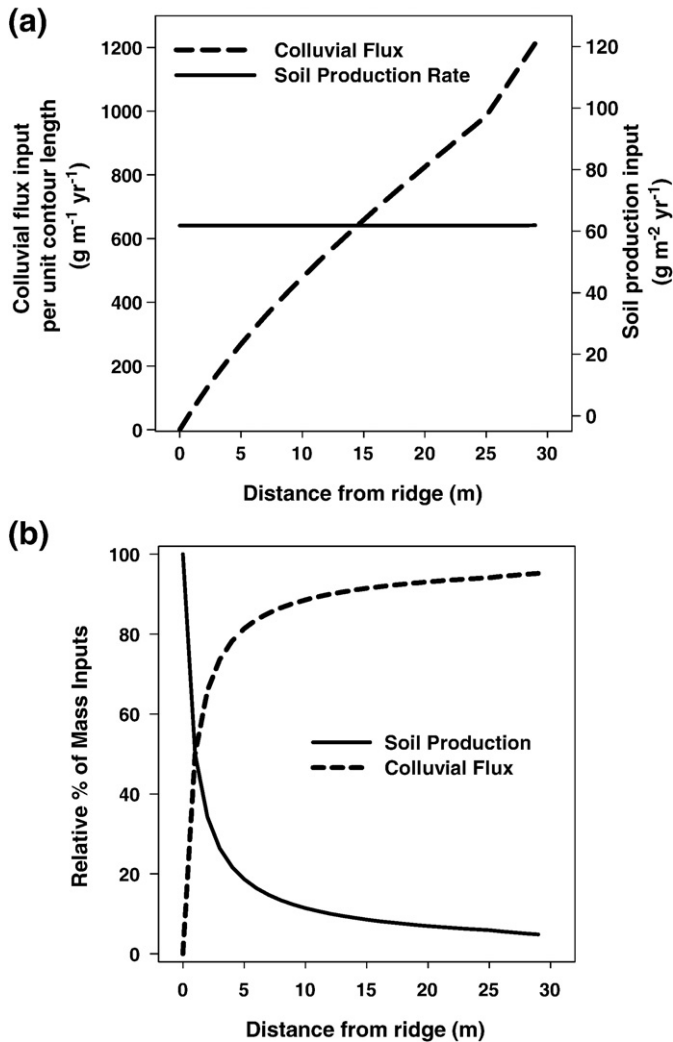


Fig. 6. Calculated physical mass fluxes of colluvial soil transport and soil production along the steady state part of the hillslope. (a) Mass inputs of soil production and colluvial soil entering soils with 1 m² surface area and (b) Relative percentage of soil production and colluvial flux in the total mass input to the soils with 1 m² surface area.

Within the steady state section, the spatial trends in the calculated Ca and P weathering rates differed significantly from those of total and major elemental weathering rates (Fig. 7d). Positive weathering rates indicated gradual enrichment of these elements in soils as the soil is transported downslope. The retention rates of Ca and P was higher in the eroding steady state slope than in the depositional area (Fig. 7d). Because biological retention of nutrient elements is a decreasing function of depth in soils, the thick depositional soil may be less efficient at retaining Ca and P. Previous studies have found that organic carbon contents of the depositional soil decreased from 3–4% at the top 0–5 cm to below 1% at the depth of ~50–60 cm at the site (Yoo et al., 2005a, 2006), reflecting the decreasing biological activity with increasing soil depth. The convex slope, however, does not have the deep soil zone (Fig. 4) with low carbon contents (<1%) (Yoo et al., 2005a, 2006). Despite the significantly lowered Ca and P retention rates in the depositional slope (Fig. 7d), its soil is still significantly enriched in Ca and P relative to the underlying saprolite (Fig. 5g and h) because of the continuous influx of soil enriched in Ca and P from upslope. Therefore, the retention rate and topographic distribution of nutrient elements are tightly controlled by the geomorphic processes shaping the hillslope's morphology.

4.6. Contribution of soil chemical weathering to landscape denudation

In the eroding steady state hillslope, chemical weathering removed soil mass at an average rate of 3.8 g m⁻² yr⁻¹, which is approximately 6% of the averaged soil production rate of 64 g m⁻² yr⁻¹. On the eroding slope, soil formation is thus largely driven by physical breakdown of parent material and its subsequent mixing and transport. However, mineral dissolution and leaching, which is largely a function of colluvial flux, result in soil chemical weathering rates that systematically vary with topographic position (Fig. 7) and impart a geochemical variation along the hillslope (Fig. 5).

Approximately 1200 g m⁻¹ yr⁻¹ of soil mass erodes from the convex slope and enters the transient slope (Fig. 6a). At this rate, it would have taken ~44 Kyr for the sedimentation to create the depositional soils. Over this time span, about 1.5 g m⁻² of mass has been annually lost via chemical weathering in the depositional area (Fig. 7a). When integrated over the depositional slope, this is ~60 g m⁻¹ yr⁻¹ of mass loss rate or about 5% of the sediment input from the convex upslope.

These rates of chemical weathering and their contribution to mass removal are the lowest among the previously reported long-term values from actively eroding upland landscapes. This is particularly interesting given the active tectonic history of the study site. In a eucalyptus-grass hillslope in New South Wales, Australia, the hillslope-averaged soil chemical weathering rate was 21 g m⁻² yr⁻¹ or 40% of the soil production (Yoo et al., 2007). In a nearby but wetter hillslope sharing similar bedrock, Green et al. (2006) reported Si weathering rates ranging from 12 to 20 g m⁻² yr⁻¹ and concluded that chemical weathering had accounted for 35–55% of the total denudation. Riebe et al. (2004) compiled watershed denudation rates and chemical weathering rates from granitic landscapes spanning a wide range of climate. According to their data, an average chemical weathering rate is ~10 g m⁻² yr⁻¹ which is ~17% of the averaged soil production rate. In a steep headwater catchment in Oregon Coastal Range, Anderson et al. (2002) reported a silicon weathering rate of 10.7 ± 7.1 g m⁻² yr⁻¹.

These previously studied sites, compared to Tennessee Valley, are underlain by bedrock or saprolite with significantly greater abundances of weatherable minerals. At our site, in both soil and saprolite, ~40% of the masses are accounted for by weathering resistant quartz. Plagioclase, which is the only primary mineral species other than quartz with a significant presence, is 10–20% of the soil and saprolite mass. In comparison, the soil formed from granodiorite in Australia (Yoo et al., 2007) was composed of 23% of K-feldspar, ~10% of Na-plagioclase, and 4% biotite (Yoo, unpublished data). Among the sites surveyed in Riebe et al. (2004), the quartz diorite bedrock at Panola Mountain, GA, USA contained plagioclase (32%), K-feldspar (21%), and biotite (13%) (White et al., 2001), and Rio Icacos, Puerto Rico was underlain by quartz diorite with ~60% plagioclase (Riebe et al., 2003a). Lastly, bedrock at the head water catchment in Oregon Coastal range (Anderson et al., 2002) is greywacke sandstone with significant (~40%) contributions from easily weatherable feldspars and volcanic fragments (Anderson and Dietrich, 2001). Therefore, low soil chemical weathering rates at Tennessee Valley are at least partly due to a low abundance of weatherable minerals in the parent material.

Additionally, at Tennessee Valley, ~40% of both soil and saprolite is occupied by secondary phyllosilicate minerals (see Section 4.2), indicating that clay minerals in soils are entirely inherited from the saprolite via physical breakdown of the saprolite. It is also likely that the significant portion of the saprolite clay is originated from the clay-rich greywacke sandstone. Likewise, in an adjacent hillslope within Tennessee Valley that share virtually identical soils and hillslope morphology (for the site information, see Sanderman et al., 2009), the amounts of amorphous and crystalline iron oxides (quantified by the difference between the Fe pools extracted by dithionite citrate and ammonium oxalate) were found to vary from 1.4 to 2.5% (Fig. 8). Soils developing on clay-free parent materials accumulate such high contents

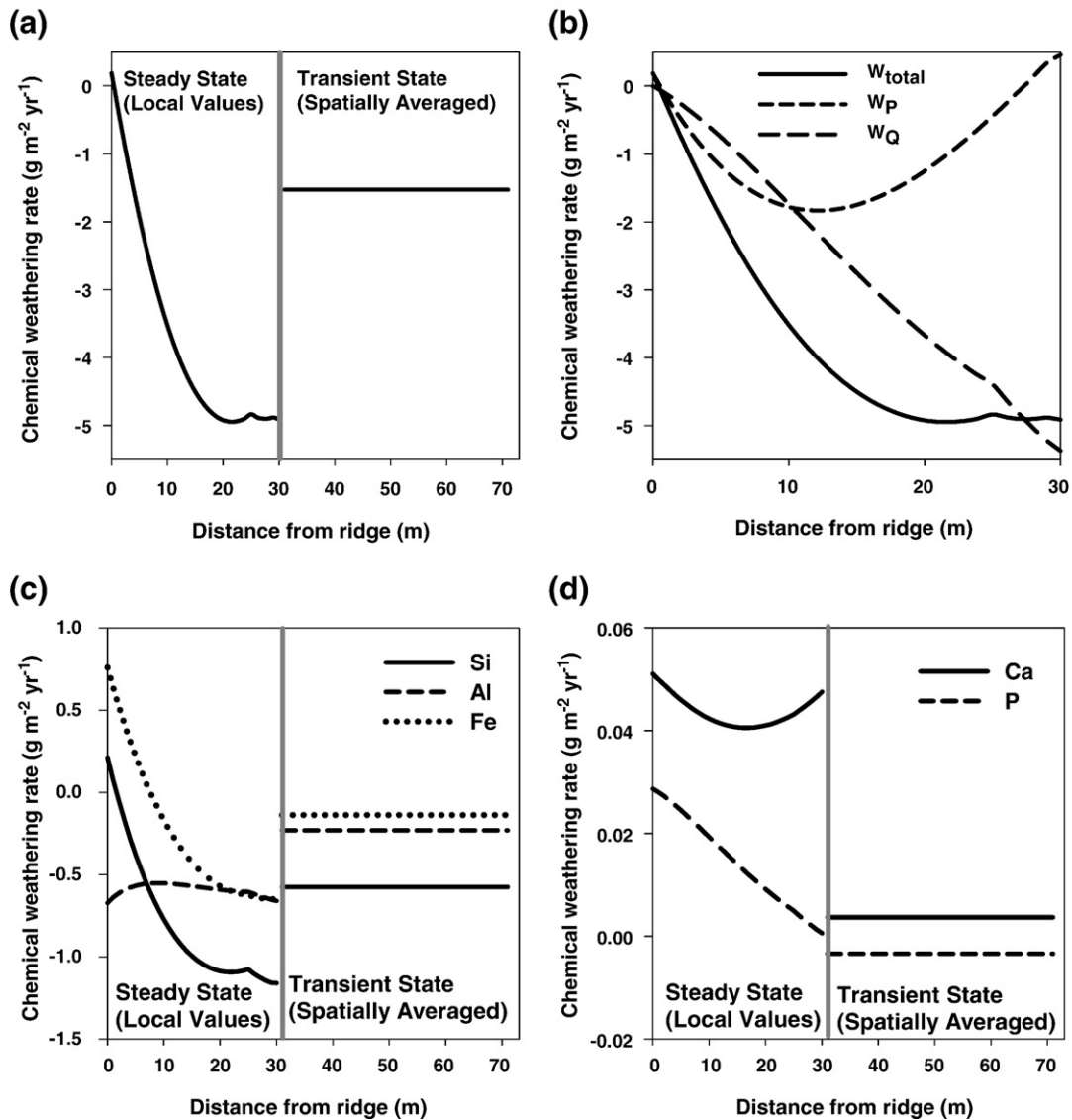


Fig. 7. Chemical weathering rates in the colluvial soil. The rates are calculated with steady state solution for the convex slope (Eqs. (3a)–(3c)), which resulted in continuous local values along the transect (Eqs. (1a) and (1b)). In contrast, in the depositional area, spatially averaged chemical weathering rates were calculated (Eqs. (4a) and (4b)). (a) Total chemical weathering rate (W_{total}) over the entire hillslope transect. (b) Enlarged steady state solution of total chemical weathering rate (W_{total}), chemical weathering rates associated with soil production (W_P) and with colluvial flux (W_Q) within the convex hillslope. (c) elemental chemical weathering rates of Si, Al, and Fe, and (d) Ca and P. Negative values indicate the mass losses via chemical weathering, while the positives represent the mass gain via precipitation. Grey vertical lines represent the boundary between the convex and planar parts of the hillslope (Fig. 4).

of clay and pedogenic iron oxides over time lengths that greatly exceed the soil residence time at Tennessee Valley hillslopes. Along a soil chronosequence formed on clay poor beach sand in coastal California, only soils with the age of 240 Kyrs accumulated similar clay and pedogenic iron oxide contents (Merritts et al., 1991). Abundant clay and iron oxides in the soil, which were inherited from the saprolite, may have contributed to the slow chemical weathering rate at Tennessee Valley. In a comprehensive review of mineral dissolution rate and soil chemical weathering as a function of time, White and Brantley (2003) documented that increased coating of primary mineral surface by secondary clay and oxide minerals and the loss of reactive surface area can explain why mineral dissolution rates decrease over time.

4.7. Topographic pattern of total chemical weathering rates within the eroding hillslope

Several explanations are possible for the pattern that the chemical weathering rate increases in the downslope direction within the

eroding hillslope. For chemical weathering to occur, an influx of weatherable minerals with reactive surfaces is required. For each mineral species, this flux can be written as the product of the following variables: (1) concentration of the mineral species, (2) specific mineral surface area of the mineral species, (3) fraction of reactive area per mineral surface area, and (4) the rate of the colluvial flux. Below these factors are examined as a function of hillslope positions.

The concentration of plagioclase varies little between the hillslope summit and the lower end of the hillslope, suggesting changes in mineral concentration do not significantly affect the chemical weathering rate. On the other hand, the reactivity of mineral surfaces may vary with topographic position as minerals are transported in the downslope direction. In the adjacent first order hillslope within Tennessee Valley (for the site information, see Sanderman et al., 2009), the pedogenic crystalline Fe oxides gradually increased in the downslope direction within the well drained shoulder and backslope areas (Fig. 8). The increased Fe oxide coating, if persists in the studied hillslope transect, may negatively affect the dissolution of primary

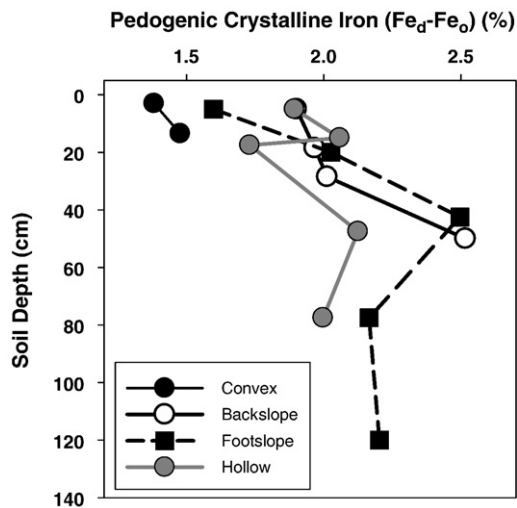


Fig. 8. Pedogenic crystalline Fe contents in soils along an adjacent hillslope transect within the Tennessee Valley. This adjacent hillslope shares virtually identical soil morphology and geochemistry and hillslope morphology (Sanderman et al., 2009) with the hillslope transect described in Fig. 3.

minerals, which contradicts the increasing chemical weathering rate in the downslope direction within the steady state hillslope (Fig. 7a). Therefore the increasing colluvial flux in the downslope direction (Fig. 6a) is likely to cause the chemical weathering rate to increase in the downslope direction.

4.8. Reduction in chemical weathering rate as the colluvial soil moves from the eroding to depositional slope

The rate of mass loss via soil chemical weathering was found to be less in the depositional slope than in the eroding area. This was somewhat unexpected because in the depositional area a greater mass of minerals (due to thicker soils) reacts with more abundant soil water. Indeed, while the fraction of plagioclase grains is not significantly different between the eroding and depositional soil pits, mineral input via sediment flux is largest in the depositional area. Furthermore, the amounts of crystalline Fe oxides, which may protect the surface of weatherable minerals from dissolution, likely decrease in the depositional slope because of seasonally reducing conditions induced by soil saturation (Fig. 8). Therefore, the reduced chemical weathering rate in the depositional area may not be explained by the prevalent view that mineral supply or reactive mineral surface area limits chemical weathering.

An alternative explanation is that subsurface water may be approaching thermodynamic equilibrium with minerals and thus suppressing weathering rates. In the eroding part of the studied hillslope, soil water has brief residence time because of the thin soil and the small contributing area and thus may not reach equilibrium with the minerals. However, in the lower convergent slope, the collection of water that has migrated through the sub-soil and saprolite as observed in an adjacent first order watershed within Tennessee Valley (Sanderman et al., 2009), may have highly elevated solute concentrations. Lastly, it appears that secondary minerals may have precipitated from soil pore water in the depositional soil. Despite relatively constant clay content over the hillslope transect, we found that clay-associated cation exchange capacity increased from 50–70 cmole/100 g clay in the eroding soil to 80–95 cmole/100 g clay in the depositional soil, indicating different clay species present in the eroding vs. depositional soils. Detailed geochemical modeling of soil solutes and minerals should be undertaken together with spatially-referenced measurements of hydrological flow paths and fluxes.

At watershed scales, a positive relationship between chemical weathering rate and mineral supply rate (ie., total denudation rate) has been recognized (Riebe et al., 2001, 2003a,b, 2004). More mechanistic investigations into the causes for this positive relationship have begun to consider the residence time of minerals within a watershed (West et al., 2005; Hren et al., 2007; Gabet and Mudd, 2009), and it has been suggested that at high erosion rates chemical weathering rates could be reduced by a lack of soil mass (e.g thin mobile soil layers) (Ferrier and Kirchner, 2008; Gabet and Mudd, 2009). To our knowledge, however, the concept of mineral supply limitation on weathering has not been applied in order to understand topographic patterns of chemical weathering. The results here suggest that mineral supply control of chemical weathering may be limited to thin soils on actively eroding areas of hillslopes. In depositional hillslopes, depending on hydrochemistry of the site, soil chemical weathering rates may be controlled by thermodynamic equilibrium between soil pore water and minerals.

5. Conclusions

Over a hillslope transect that includes both steady state and transient areas of soil thickness, this study demonstrated that soil chemical weathering rates were greatest in the lower part of the eroding hillslope and that the chemical weathering rates were significantly lower in the thick depositional soils. It was suggested that geomorphic changes in hillslopes in response to channel activities ultimately determine how the two competing controls of weathering rate, mineral supply rate vs. mineral–solute interactions, were spatially distributed over landscapes. This study also extended the data on the feedback between sediment transport and chemical weathering rate to include hillslopes underlain by clay-rich sedimentary rock. Significant amounts of clay already present in the saprolite at Tennessee Valley led to the soil that behaved like aged soils in terms of dissolution characteristics of its minerals. The calculated long-term chemical weathering rates, which are the lowest among the previously reported values from eroding landscapes, are in agreement with the growing consensus that mineral dissolution rate decreases over time as minerals' surface reactivity is reduced. Spatial patterns of Ca and P suggested that the vertical extent of biological activities, in combination with morphologic evolution of hillslopes, may have significantly modulated the topographic distribution of biologically important elements. This is because organisms compete with sediment transport and soil water fluxes in controlling the fate of these elements.

Hillslopes provide a convenient platform where the interactions among major earth surface processes of generation and transport of sediments and geochemical soil formation can be scrutinized at the process level in response to the external forcings of climate change and tectonic activity. Previous works coupling physical denudation and chemical weathering at watershed scales (Riebe et al., 2001, 2003a,b, 2004), relying on point measurements of soils, saprolites, and bedrock, have resulted in important hypotheses or observations about landscape processes. This work and others (Nezat et al., 2004; Green et al., 2006; Yoo et al., 2007) provide insight into how these processes vary with topographic position. Accurate determination of long-term chemical weathering rates at watershed scales may require or should be complemented by a toposequence approach. The next major step is to add soil solute chemistry and hydrology and the processes occurring within the underlying saprolite. However, in the absence of such comprehensive work, the soil solids on hillslopes hold great insight into what are largely unanticipated complexities.

Acknowledgements

This study is partially supported by NSF EAR0819064 grant to K. Yoo and S. Mudd. Thoughtful comments by George Hillel and an

anonymous reviewer significantly improved this paper. The authors thank Golden Gate National Recreation Area in National Park Service for their cooperation during the research.

Appendix A. Supplementary data

Supplementary data associated with this article can be found, in the online version, at doi: [10.1016/j.epsl.2009.09.021](https://doi.org/10.1016/j.epsl.2009.09.021).

References

- Amundson, R., 2004. Soil formation. In: Holland, H.D., Turekian, K.K. (Eds.), *Treatise on Geochemistry*. Elsevier Science Ltd., Oxford, UK, pp. 1–35.
- Anderson, S.P., Dietrich, W.E., 2001. Chemical weathering and runoff chemistry in a steep headwater catchment. *Hydrol. Process.* 15, 1791–1815.
- Anderson, S.P., Dietrich, W.E., Brimhall, G.H., 2002. Weathering profiles, mass-balance analysis, and rates of solute loss: Linkages between weathering and erosion in a small, steep catchment. *GSA Bull.* 114, 1143–1158.
- Anderson, S.P., von Blanckenburg, F., White, A.F., 2007. Physical and chemical controls on the critical zone. *Elements* 3, 315–319.
- Berner, R.A., 1995. Chemical weathering and its effect on atmospheric CO₂ and climate. In: White, A.F., Brantley, S.L. (Eds.), *Chemical weathering rates of silicate minerals*. Mineralogical Society of America, Washington D.C., pp. 565–583.
- Black, T.A., Montgomery, D.R., 1991. Sediment transport by burrowing mammals, Marin County, California. *Earth Surf. Proc. Land.* 16, 163–172.
- Brimhall, G.H., Dietrich, W.E., 1987. Constitutive mass balance relations between chemical composition, volume, density, porosity, and strain in metasomatic hydrochemical systems: results on weathering and pedogenesis. *Geochim. Cosmochim. Acta* 51, 567–587.
- Davis, W.M., 1892. The convex profile of bad-land divides. *Science* 20, 245.
- Dietrich, W.E., Bellugi, D.G., Sklar, L.S., Stock, J.D., Heimsath, A.M., Roering, J.J., 2003. Geomorphic transport laws for predicting landscape form and dynamics. In: Wilcock, P.R., Iverson, R.M. (Eds.), *Predictions in Geomorphology*. American Geophysical Union, Washington D.C., pp. 103–132.
- Eberl, D.D., 2003. User's Guide to Rockjock – a program for determining quantitative mineralogy from powder X-ray diffraction data. U.S. Geological Survey Open-File Report, vol. 03–78. 46 pp.
- Fernandes, N.F., Dietrich, W.E., 1997. Hillslope evolution by diffusive processes: the timescale for equilibrium adjustments. *Water Resour. Res.* 33, 1307–1318.
- Ferrier, K.L., Kirchner, J.W., 2008. Effects of physical erosion on chemical denudation rates: a numerical modeling study of soil-mantled hillslopes. *Earth Planet. Sci. Lett.* 272, 591–599.
- Furbish, D.J., Fagherazzi, S., 2001. Stability of creeping soil and implications for hillslope evolution. *Water Resour. Res.* 37, 2607–2618.
- Gabet, E.J., Mudd, S.M., 2009. A theoretical model coupling chemical weathering rates with denudation rates. *Geology* 37, 151–154.
- Gilbert, G.K., 1909. The convexity of hilltops. *J. Geol.* 17, 344–350.
- Green, E.G., Dietrich, W.E., Banfield, J.F., 2006. Quantification of chemical weathering rates across an actively eroding hillslope. *Earth Planet. Sci. Lett.* 242, 159–169.
- Heimsath, A.M., Dietrich, W.E., Nishiizumi, K., Finkel, R.C., 1997. The soil production function and landscape equilibrium. *Nature* 388, 358–361.
- Heimsath, A.M., Furbish, D.J., Dietrich, W.E., 2005. The illusion of diffusion: field evidence for depth dependent sediment transport. *Geology* 33, 949–952.
- Hren, M.T., Hilley, G.E., Chamberlain, G.P., 2007. The relationship between tectonic uplift and chemical weathering rates in the Washington cascades: field measurements and model predictions. *Am. J. Sci.* 307, 1041–1063.
- Humphreys, G.S., Wilkinson, M.T., 2007. The soil production function: a brief history and its rediscovery. *Geoderma* 139, 73–78.
- Kurtz, A.C., Derry, L.A., Chadwick, O.A., Alfano, M.J., 2000. Refractory element mobility in volcanic soils. *Geology* 28, 683–686.
- Montgomery, D.R., 1999. Erosional processes at an abrupt channel head: implications for channel entrenchment and discontinuous gully formation. In: Darby, S.E., Simon, A. (Eds.), *Incised river channels*. John Wiley & Sons Ltd, pp. 247–276.
- Montgomery, D.R., Dietrich, W.E., 1989. Source areas, drainage density, and channel initiation. *Water Resour. Res.* 25, 1907–1918.
- Montgomery, D.R., Dietrich, W.E., 1995. Hydrological processes in a low-gradient source area. *Water Resour. Res.* 31, 1–10.
- Mudd, S.M., Furbish, D.J., 2004. The influence of chemical denudation on hillslope morphology. *J. Geophys. Res. -Earth Surf.* 109, F02001. doi:10.1029/2003JF000087.
- Mudd, S.M., Furbish, D.J., 2005. Lateral migration of hillcrests in response to channel incision in soil-mantled landscapes. *J. Geophys. Res. -Earth Surf.* 110, F04026. doi:10.1029/2005JF000313.
- Mudd, S.M., Furbish, D.J., 2006. Using chemical tracers in hillslope soils to estimate the importance of chemical denudation under conditions of downslope sediment transport. *J. Geophys. Res. -Earth Surf.* 111, F02021. doi:10.1029/2005JF000343.
- Mudd, S.M., Furbish, D.J., 2007. Responses of soil-mantled hillslopes to transient channel incision rates. *J. Geophys. Res. -Earth Surf.* 112, F03518. doi:10.1029/2006JF000516.
- NCDC, 2007. Climatic data summary for station #4500 Kentfield, CA. Cited 15 April 2007. <http://www.ncdc.noaa.gov/oa/ncdc.html>.
- Nezat, C.A., Blum, J.D., Klaue, A., Johnson, C.E., Siccama, T.G., 2004. Influence of landscape positions and vegetation on long-term weathering rates at the Hubbard Brook Experimental Forest, New Hampshire, USA. *Geochim. Cosmochim. Acta* 68, 3065–3078.
- O'Farrell, C.R., Heimsath, A.M., Kaste, J.M., 2007. Quantifying hillslope erosion rates and processes for a coastal California landscape over varying timescales. *Earth Surf. Proc. Land.* 32, 544–560.
- Porder, S., Paytan, A., Vitousek, P.M., 2005. Erosion and landscape development affect plant nutrient status in the Hawaiian Islands. *Oecologia* 142, 440–449.
- Porder, S., Vitousek, P.M., Chadwick, O.A., Chamberlain, C.P., Hilley, G.E., 2007. Uplift, erosion, and phosphorus limitation in terrestrial ecosystems. *Ecosystems* 10, 158–170.
- Prosser, I.P., Dietrich, W.E., 1995. Field experiments on erosion by overland flow and their implication for a digital terrain model of channel initiation. *Water Resour. Res.* 31, 2867–2876.
- Prosser, I.P., Dietrich, W.E., Stevenson, J., 1995. Flow resistance and sediment transport by concentrated overland flow in a grassland valley. *Geomorphology* 13, 71–86.
- Raymo, M.E., Ruddiman, W.F., 1992. Tectonic forcing of late Cenozoic climate. *Nature* 359, 117–122.
- Reneau, S.L., Dietrich, W.E., Donahue, D.J., Jull, A.J.T., Rubin, M., 1990. Late Quaternary history of colluvial deposition and erosion in hollows, central California Coast Range. *Geol. Soc. Am. Bull.* 102, 969–982.
- Riebe, C.S., Kirchner, J.W., Granger, D.E., Finkel, R.C., 2001. Minimal climatic control on erosion rates in the Sierra Nevada, California. *Geology* 29, 447–450.
- Riebe, C.S., Kirchner, J.W., Finkel, R.C., 2003a. Long-term rates of chemical weathering and physical erosion from cosmogenic nuclides and geochemical mass balance. *Geochim. Cosmochim. Acta* 67, 4411–4427.
- Riebe, C.S., Kirchner, J.W., Finkel, R.C., 2003b. Sharp decrease in long-term chemical weathering rates along an altitudinal transect. *Earth Planet. Sci. Lett.* 218, 421–434.
- Riebe, C.S., Kirchner, J.W., Finkel, R.C., 2004. Erosional and climatic effects on long-term chemical weathering rates in granitic landscapes spanning diverse climate regimes. *Earth Planet. Sci. Lett.*
- Roering, J.J., Kirchner, J.W., Dietrich, W.E., 1999. Evidence for nonlinear, diffusive sediment transport on hillslopes and implications for landscape morphology. *Water Resour. Res.* 35, 853–870.
- Sanderman, J., Lohse, K.A., Baldock, J.A., Amundson, R., 2009. Linking soils and streams: sources and chemistry of dissolved organic matter in a small coastal watershed. *Water Resour. Res.* 45, W03418. doi:10.1029/2008WR006977.
- Wahrhaftig, C., 1984. Structure of the Marin Headlands block, California: a progress report. *Francisc. Geol. North. Calif.* 43, 31–50.
- Wakabayashi, J., 1999. Distribution of displacement on and evolution of a young transform fault system: the northern San Andreas fault system, California. *Tectonics* 18, 1245–1274.
- West, A.J., Galy, A., Bickle, M., 2005. Tectonic and climatic controls on silicate weathering. *Earth Planet. Sci. Lett.* 235, 211–228.
- White, A.F., Brantley, S., 2003. The effect of time on the weathering of silicate minerals: why do weathering rates differ in the laboratory and field? *Chem. Geol.* 202, 479–506.
- White, A.F., Bullen, T.D., Schulz, M.S., Blum, A.E., Huntington, T.G., Peters, N.E., 2001. Differential rates of feldspar weathering in granitic regoliths. *Geochim. Cosmochim. Acta* 65, 847–869.
- Yoo, K., Mudd, S.M., 2008a. Toward process-based modeling of geochemical soil formation across diverse landforms: a new mathematical framework. *Geoderma* 146, 248–260.
- Yoo, K., Mudd, S.M., 2008b. Discrepancy between mineral residence time and soil age: implications for the interpretation of chemical weathering rates. *Geology* 36, 35–38.
- Yoo, K., Amundson, R., Heimsath, A.M., Dietrich, W.E., 2005a. Erosion of upland hillslope soil organic carbon: coupling field measurements with a sediment transport model. *Global Biogeochem. Cycles* 19, GB3003. doi:10.1029/2004GB002271.
- Yoo, K., Amundson, R., Heimsath, A.M., Dietrich, W.E., 2005b. A process based model linking pocket gopher (*Thomomys bottae*) activity to sediment transport and soil thickness. *Geology* 33, 917–920.
- Yoo, K., Amundson, R., Heimsath, A.M., Dietrich, W.E., 2006. Spatial patterns of soil organic carbon on hillslopes: integrating geomorphic processes and the biological C cycle. *Geoderma* 130, 47–65.
- Yoo, K., Amundson, R., Heimsath, A.M., Dietrich, W.E., Brimhall, G.H., 2007. Integration of geochemical mass balance with sediment transport to calculate rates of soil chemical weathering and transport on hillslopes. *J. Geophys. Res. -Earth Surf.* 112, F02013. doi:10.1029/2005JF000402.